

Buckling of Anodic Films on Aluminum

Determination of Plastic Deformation Energy of Coatings

O. Teschke,^{*a} M. U. Kleinke,^a and F. Galembeck

Instituto de Física^a and Instituto de Química, UNICAMP, 13081-970, Campinas, SP, Brasil

ABSTRACT

The mechanical instability of oxide layers on anodized aluminum generates a regular arrangement of straight lines parallel to the cylindrical electrode axis. This is analyzed using Euler's equation for buckling of thin cylindrical shells under compressive forces, due to volume expansion concurrent with metal-oxide formation. The coating critical stress is determined as well as the energy dissipated by plastic deformation of the anodic coating. Most of the energy associated with compressive stress of the oxide film is dissipated by plastic deformation.

It is natural to inquire about the stresses and strains which exist in anodic films formed on metallic surfaces.^{1,2} Building up these films involves many steps, which include the reactions of oxide formation, nucleation and growth of its colloidal particles, their aggregation, film formation and aging, and the events during the drying process. Aggregation, aging, water removal, and oxide condensation reactions all introduce some degree of stress in the film.

The ultimate thickness to which an oxide film may grow before it cracks, *i.e.*, the protective thickness, depends on its ability to withstand or relieve the stresses which may arise during growth. If the accumulated stress exceeds the strength of the film, cracking or detachment will occur, resulting in an increase in the metal corrosion rate. In order to improve the corrosion resistance by increasing the protective thickness of the oxide film, data are required on the stresses which are produced during film growth.

Stress in anodic aluminum films has been measured by Bradhurst and Leach³ and more recently by Leach and Pearson.^{4,5} The stresses have been measured by clamping the upper end of a thin foil of the metal and observing the motion of the lower end. The formula used for calculating stress in terms of the end deflection of the beam was derived by various workers. The earliest analysis of Stoney⁶ assumed that Young's moduli of the film and the substrate were identical and that the stress was isotropic. The theory used to derive Stoney's equation is limited in its applicability as observed by Klokholm⁷ and Hoffman.⁸ Brenner and Senderoff⁹ have reviewed Stoney's derivation in some detail and obtained formulas to cover all the common experimental arrangements. They considered the effect of different elastic moduli in film and substrate. A detailed discussion of a more exact derivation of the relationship of film and substrate can be found in Ref. 2. High-temperature-oxidation-induced stresses and their effects on the behavior of oxide films on silicon have been studied by Hsueh and Evans.¹⁰ The energetics of crack formation will not be discussed in this paper and may be found in Ref. 11, 12.

This paper describes experiments designed to evaluate the stresses in anodic films under different conditions of growth and gives some observations which support the concept that plastic deformation of a growing oxide film may occur at room temperature. Stress dissipation by plastic deformation is evaluated indirectly by evaluating the compressive energy of the oxide film, following Euler's equation for buckling in thin cylindrical shells

Experimental

A special cell with an axially symmetric current distribution was built in order to generate a radially isotropic stress distribution within the electrode anodic coating. The test cell is schematically shown in Fig. 1.¹³ The cell walls and cover are made of poly(tetrafluoroethylene) (PTFE). The electrolytic cell was operated at atmospheric pressure. The working electrodes were 4 cm long aluminum rods with a diameter of 0.46 cm. The length of the electrode exposed to the solution is adjustable from 2 mm to 2 cm by varying the

distance between two PTFE O rings; the counterelectrode is a concentric cylindrical platinum mesh creating a radial current distribution. The radial distance between the two concentric electrodes is 1.5 cm. The specimens were prepared from the same aluminum wire (commercial grade 99.2% pure, supplied by Alcan). They were abraded with emery paper (grid 600), polished with diamond paste (through 0.5 μm), and annealed at 300°C for 2 h in a 13 Pa atmosphere. The surfaces of the specimens were immersed in a chromic-phosphoric acid solution (20 g/liter H_2CrO_4 and 35 ml/liter H_3PO_4) for 5 min at 80°C, washed with distilled water, and anodized. Anodic oxide films were formed at various current densities in a 7.5% sulfuric acid solution thermostated at 25°C. During film growth, *in situ* observation was made using an Olympus Model 52-TR-BR stereoscope. The anodization was stopped when the striae arrangement appeared on the electrode surface. The electrolytic solution was prepared with twice-distilled water and sulfuric acid (analytical grade). The galvanostat is a PAR Model 273A galvanostat/potentiostat. After their removal from the electrolyte, a few of the electrodes were rinsed with distilled water, dried, and introduced into a vacuum chamber, and a gold layer of about 150 Å was evaporated over their surfaces. Then they were examined in a JEOL TS-300 scanning electron microscope.

The thickness h of aluminum oxide formed during the anodization time Δt is given by Faraday's law $h = i\Delta tM/3F\rho(1 + \alpha)$, where i is the current density, M is the molecular weight, ρ is the density of aluminum, F is the Faraday constant, and α is the oxide linear-expansion coefficient. The thickness was also measured by scanning electron mi-

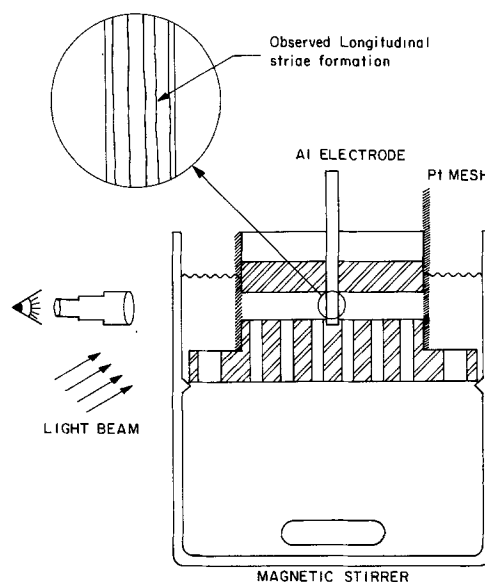


Fig. 1. Schematic diagram of the test cell.

* Electrochemical Society Active Member.

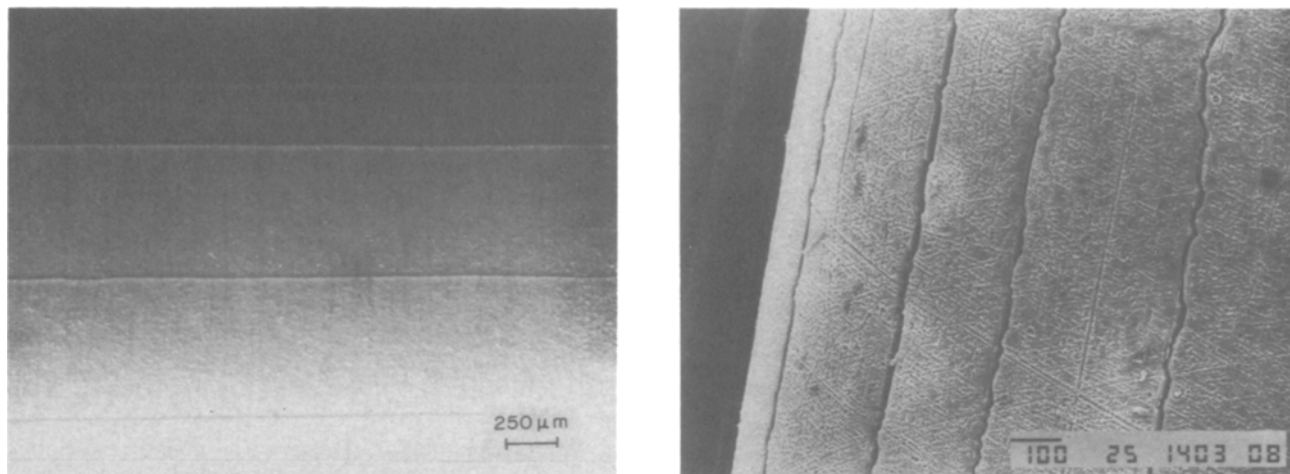


Fig. 2. Optical (a, left) and SEM (b, right) micrographs showing the failure by buckling of the oxide film which resulted in a pattern of striae axially along the periphery of the electrode. (a) Buckling of the anodic film, $I = 4 \text{ A} \cdot \text{cm}^{-2}$, $t = 0.8 \text{ s}$; (b) longitudinal striae in the outer perimeter of the oxide film, $I = 0.1 \text{ A} \cdot \text{cm}^{-2}$, $t = 600 \text{ s}$, and $\phi = 0.46 \text{ cm}$.

crosscopy (SEM) and optical microscopy of the transverse cross section of the anodized cylinders.

Results

We carried out several preliminary experiments. At first, we anodized various plane surfaces. For anodized plane surfaces without lateral constraints, there is no compression due to oxide formation and consequently no pattern was observed on these surfaces. A special arrangement of cell (cylinders axially symmetric) was then built in order to generate an isotropic stress distribution in the anodic film.

As the aluminum substrate is anodized, the compressive stress in the growing oxide film causes deformation. Figure 2a and b shows a series of fringes on an oxide film along the outer periphery of the aluminum rod. These fringes correspond to the maximum vertical displacement of the corrugated oxide film, and they form a regular arrangement of straight lines parallel to the rod axis. The patterns are formed only when the anodization charge is larger than a critical value. When the electrode charge is smaller than this value, the film surface remains smooth. For each current density, the critical charge density is determined *in situ* by the observation of the electrodes using an optical stereoscope. When the critical thickness of oxide is reached, the striae arrangement appears on the electrode surface, and the process is stopped. The number of striae is counted *in situ*, and the film thickness is determined by measuring the total charge passed.

A few of the samples were later observed by SEM. The effect of the film drying under UHV and possible heating of the film during Au deposition modified the cracks' dimensions. A systematic study of these effects was not fully carried out. The effect of the drying process on the striae formation is displayed in Fig. 3, which shows the crack at the top of the ridge. This micrograph shows that the crack width after drying under UHV is approximately $10 \mu\text{m}$.

We have carried out several experiments anodizing aluminum rods with some additives added to the electrolytic medium. Sucrose, ethylene glycol, and glycerine were added to aqueous sulfuric acid to change the characteristics of the film, resulting in changes in striae numbers as shown in Table I. The effect of ethylene glycol on both oxide and crack structures is shown in Fig. 4a and b.

The experimental results for the number of striae in the film obtained under various current densities and time intervals are shown in Table II.

Discussion

Stresses in growing oxide films arise from the volume change which occurs when a specific quantity of a metal is converted into metal oxide, and this may cause the buckling of the anodic film especially when the oxide forms on surfaces with large curvatures.

We did not observe buckling under axial compression, which should generate rings around the cylinder electrode. This may be understood considering that we used PTFE O rings to limit the anodization region of the aluminum cylinder. These O rings do not impose a rigid enough boundary to the (axial) oxide expansion. The observed striae formation is shown schematically in Fig. 5, as well as the tangential stress component responsible for the measured displacements of the oxide coating.

A stress analysis of anodic-film buckling has to consider energy dissipation during plastic deformation of a viscoelastic coating since most oxides are susceptible to viscoelastic deformation during anodization.¹¹ However, important physical insights can be gained from elastic analyses.¹⁰ In this paper the stress is calculated using an elastic analysis. Initially, we have a thin oxide layer with a perimeter equal to $2\pi R$, which is compressed due to its density being lower than that of aluminum metal. The stress is assumed uniform in the film and is given by Hooke's law. The linear elastic strain coefficient α is calculated by

$$\alpha = \left(\frac{V_{\text{oxide}}}{V_{\text{metal}}} \right)^{1/3} - 1 = (1 + \Delta V)^{1/3} - 1 \quad [1]$$

where $V_{\text{oxide}}/V_{\text{metal}}$ is the oxide/metal volume ratio. For small volume-expansion coefficients, ΔV may be approximated by $\alpha = \Delta V/3$. For anodized aluminum films, the ratio of the oxide volume to the metal volume is 1.28,³ which corresponds to a linear strain α of 0.085; since the volume expansion is significant, we used Eq. 1 and not its approximation

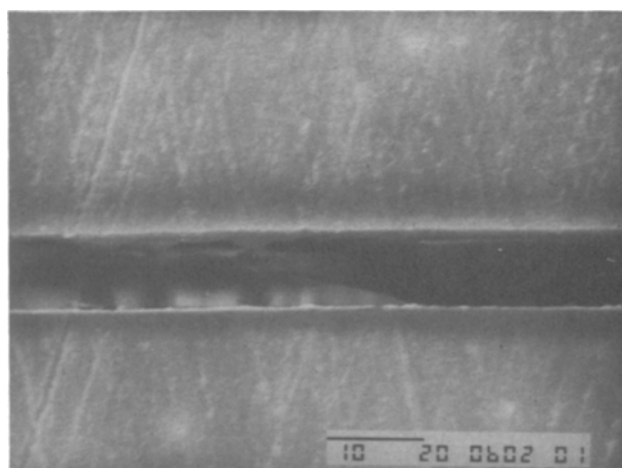


Fig. 3. Cracks formed at the top of the striae shown in Fig. 2a.

Table I. Effect of electrolyte additives on the number of striae formed in the anodic oxide films for sulfuric acid at 7.5% and $I = 50 \text{ mA} \cdot \text{cm}^{-2}$.

Solution	Anodization time (s)	Number of striae	Critical thickness (μm)
Pure	986	16	18.5
+2% Sucrose	1046	24	19.6
+2% Glycerine	988	28	18.5
+10% Ethylene Glycol	1362	25.5	

$\alpha = \Delta V/3$. If there were no viscoelastic deformation during the anodization process, the strain in the film would be given by α . To verify this assumption we measured *in situ* the stress during the anodization process. This is performed by using the Euler method for critical-strain calculation.

Euler Critical-Strain Calculation for Thin Films

Photographs similar to the ones displayed in Fig. 2a and b show that cylindrically strained oxide layers can develop ripples with wavelengths $\lambda_m = 2\pi R/m$, where R is the aluminum rod radius and $m = 2, 4, 6, \dots$, for an oxide thickness greater than a critical value. Since there is striae formation only after a certain amount of charge passes through the electrode, the critical oxide-layer thickness has to be determined. For each current density, a critical thickness is determined by observation of the electrode surface with an optical stereoscope. When the critical thickness of the oxide is reached, the arrangement of striae appears on the electrode surface, and the process is stopped. In order to determine the strain in the oxide film from the measured critical thickness, an expression derived by Euler was used.¹⁴ This expression describes the mechanical instability of a thin cylindrical shell under compression forces.¹⁴ It gives solutions for radial displacements, representing deflections of the cylindrical surface as shown in Fig. 5b. In the case of a long circular cylindrical shell uniformly compressed, the critical value of the buckling strain ϵ_c is given by

$$\epsilon_c = \frac{h^2(m^2 - 1)}{12(1 - \nu^2)R^2} \quad [2]$$

where h is the oxide critical thickness and ν is Poisson's ratio. The values of the strain, ϵ_c , which causes film buckling, for various current densities are shown in Fig. 6. As an illustration, let us determine the stress for a coating anodized with a $50 \text{ mA} \cdot \text{cm}^{-2}$ current density during 1010 s. After buckling, this coating shows 16 striae. The calculated film stress for $E = 42 \text{ GPa}$,³ obtained from Eq. 2 for $R = 0.23 \text{ cm}$, $\nu = 0.17$, and $h = 19 \mu\text{m}$ is $\epsilon_c = 0.006$, in agreement with the value shown in Ref. 3 for low current densities ($\sim 5 \text{ mA} \cdot \text{cm}^{-2}$).

Euler's expression was derived for thin cylindrical shells under compressive forces.¹⁴ A more rigorous derivation is necessary taking into account the film/substrate adhesion, which, however, is not yet available and is not the objective of this paper. The following calculation suggests that this is a reasonable approximation. Let us assume that the stored mechanical energy in the film due to the anodization of the aluminum is equal to the surface energy at buckling.^{7,11,12} The stored stress energy in anodic aluminum films with a thickness h is $E\epsilon^2h$, where ϵ is obtained from the Pilling/Bedworth ratio (1.28), giving a linear expression coefficient (strain) of 0.086. For $h = 10 \mu\text{m}$, $E\epsilon^2h = 3106$ which results in $\gamma = 1553 \text{ N/m}$. This value is three orders of magnitude larger than the accepted value of $\sim 2 \text{ N/m}$.¹¹ However, if we calculate the adhesion energy value using the critical stress obtained by Euler's expression, we obtain values in close agreement with the values found in the literature.⁹

Our approximation has previously been used by Hsueh and Evans¹⁰ and Evans and Hutchinson.¹⁵ They describe the mechanism of the delamination and spalling of compressed coatings for a delaminated circular region with a radius a . They have shown, by dimensional considerations, that the strain energy change in the substrate, as a result of the stress redistribution due to buckling, is on the order of h/a (h film thickness) times that from the buckled portion of the film, and it consequently was neglected. Similarly, the radial deflection of the substrate, where it joins the buckled film at $r = a$, is of the order h/a times the misfit. Thus, the deflection of the substrate due to buckling of the film was also neglected. The elastic energy stored in the buckled plate was then equal to the work done by the edge load to force the plate back to an edge radius, a . They concluded that the plate will undergo buckling if the compressive edge stress (averaged through the thickness) exceeds the critical buckling stress for a clamped circular plate, $\sigma_c \sim E/12(1 - \nu^2)(h/a)^2$, which is equivalent to our expression (Eq. 2) applied to cylindrical shells.

Plastic Deformation Energy

Brittle materials are those which do not show large-scale plastic flow before failing by rupture. However even very brittle materials exhibit some plasticity under stress so that part of the stressing energy is always dissipated. The energy released per unit length, called plastic dissipated energy, W_{PD} , is equal to the difference between the compression energy induced by volume increase during oxide formation and the energy calculated by Euler's critical value, *i.e.*, $(E/2) \cdot \epsilon_{\text{Euler}}^2$, as follows

$$W_{PD} = (E/2)(\alpha^2 - \epsilon_{\text{Euler}}^2) \cdot V_f$$

where V_f is the film volume per unit length and equal to $2\pi Rh$. This is illustrated in Fig. 7, which displays the exper-

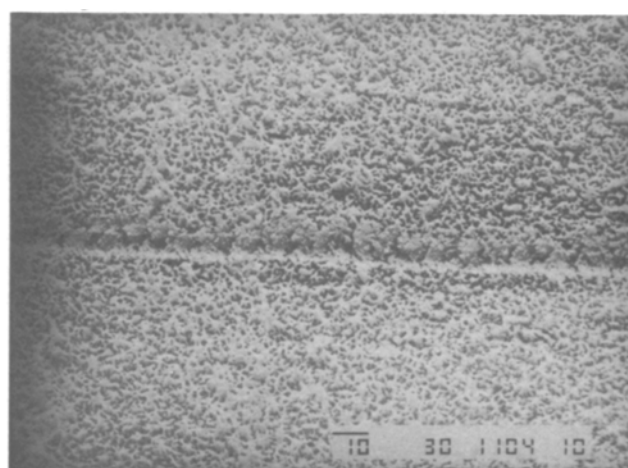
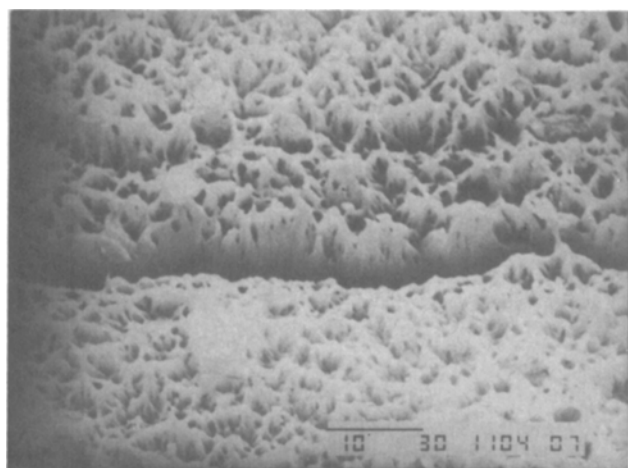
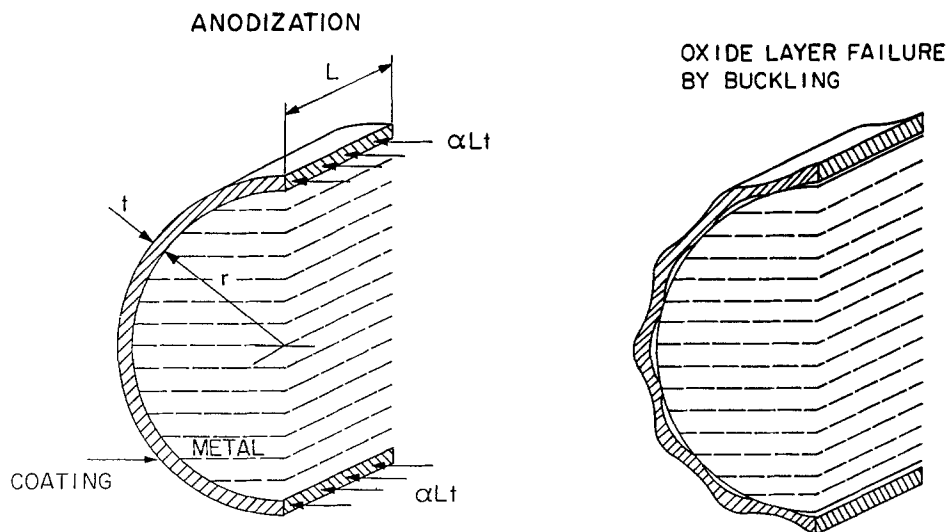


Fig. 4. The effect of ethylene glycol on both oxide and crack structure (a, left) 10%, (b, right) 20% w/w ethylene glycol in the electrolyte.

Fig. 5. (a) Schematic diagram showing the coating tangential stress component during anodization of aluminum. (b) Schematic illustration showing the patterned structure observed after oxide-layer failure by buckling.



imental results (Table II), by dots, corresponding to Euler's critical energy at buckling, and the compressive energy, by a continuous line. The difference between the compressive energy and Euler's critical energy is the plastic energy dissipated during film-formation process. We observe that the energy released at the buckling process is a small fraction of the compressive energy, approximately three orders of magnitude smaller than the total compressive energy built into the film during its growth. Consequently, plastic dissipation is very effective during the growth of anodic alu-

minum coatings. The dissipated energy is plotted in Fig. 8 as a function of current density. High current densities produce coatings in which plastic energy dissipation is less than in coatings obtained at lower current densities. This may be understood considering that at higher deposition rates the oxide has less time to undergo plastic deformation and thus to dissipate mechanical energy.

Sucrose, ethylene glycol, and glycerine were added to aqueous sulfuric acid to change the characteristics of the film. This resulted in changes in striae numbers, which are shown in Table I. Both glycerine and sucrose when added to the electrolyte produce larger numbers of striae in the oxide coating, while ethylene glycol addition requires a large thickness in order to produce mechanical instability. This may be understood considering that sucrose as well as glycerine, is a polyhydroxylated, stiff molecule which should increase the rigidity of the aluminum oxide film by cross-linking aluminum ions and consequently should increase its stiffness. Ethylene glycol is a bidentate, flexible ligand, which can be expected to replace water by introducing flexible bonds among aluminum ions. Consequently, the plastic-dissipated energy in the films is substantially modified by these electrolyte additives.

The plastic nature of the growing anodic film arises from its colloidal nature. This characteristic allows radial, diffusive mass transfer as well as stressing energy storage during film formation.

Conclusions

The mechanical instability of the anodic oxide layer in cylindrical wires is associated with the stress-produced volume expansion concurrent with oxide formation during anodization. The mechanical instability of this film was analyzed using Euler's method applied to thin cylindrical shells under compressive forces. This method allows us to

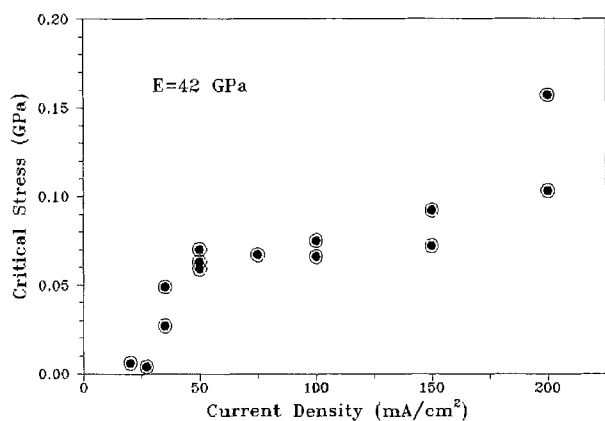


Fig. 6. Critical stress values calculated by Euler's expression, as a function of anodization current density.

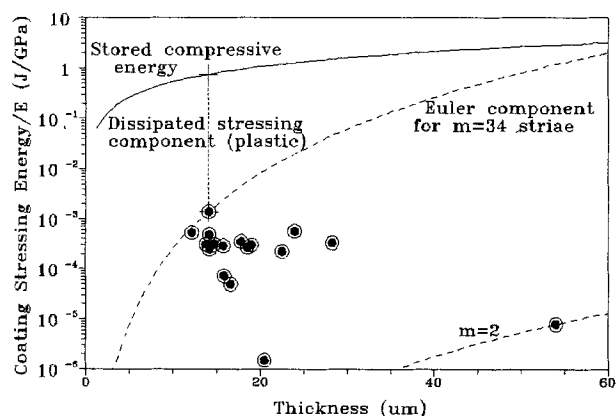


Fig. 7. Experimental values of the stressing energy, given by dots, divided by the Young modulus E in the coating calculated following Euler's method. The stored compressive energy divided by E is given by the continuous line ($\alpha^2/2$) as a function of thickness. The vertical bar shows the stressing energy dissipated within a coating that buckled forming 34 striae.

Table II. Anodic film data. The parameters are: current density I ($\text{mA} \cdot \text{cm}^{-2}$), the estimated critical oxide-film thickness h (μm), and the measured number of striae m .

I ($\text{mA} \cdot \text{cm}^{-2}$)	Anodization time (s)	Number of striae	Critical thickness (μm)
20	3765	2	54.0
27	2019	4	20.4
35	1263	12	16.6
35	1714	12	22.5
50	1012	16	19.0
50	986	16	18.5
75	563	14	15.8
75	560	20	15.8
100	378	22	14.2
100	368	24	13.8
150	262	22	14.7
200	162	32	12.2

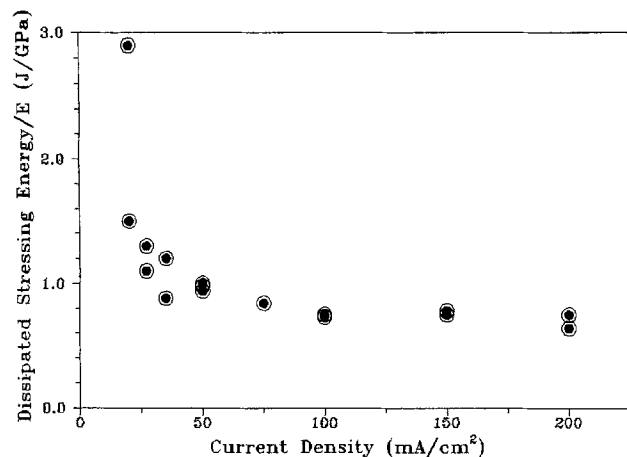


Fig. 8. Dissipated stressing energy in the film due to plastic deformation as a function of current density.

determine the film stress *in situ* and the energy dissipated during the coating formation. Plastic flow is an effective stress-dissipation mechanism in anodic aluminum oxide coatings. However, thicker layers may store enough stressing energy to cause film failure by buckling.

Acknowledgments

The authors thank José Roberto de Castro and Luis Orivaldo Bonugli for technical assistance, and are grateful to CNPq and FAEP for financial support.

Manuscript submitted Oct. 9, 1992; revised manuscript received Feb. 1, 1993.

Dr. O. Teschke assisted in meeting the publication costs of this article.

REFERENCES

1. D. A. Vermilyea, *This Journal*, **110**, 345 (1963).
2. D. S. Campbell, in *Handbook of the Thin Film Technology*, L. I. Maissel and R. Glang, Editors, pp. 12-29, McGraw-Hill, Inc., New York (1970).
3. D. M. Bradhurst and J. S. L. Leach, *This Journal*, **113**, 1245 (1966).
4. L. C. Archibald and J. S. L. Leach, *Electrochim. Acta*, **22**, 15 (1977).
5. J. S. L. Leach and B. R. Pearson, *Corros. Sci.*, **28**, 43 (1988).
6. C. G. Stoney, *Proc. Roy. Soc. London A*, **32**, 172 (1909).
7. E. Klokholm, *IBM Res. Rept.*, RC 1352 (Feb. 1965).
8. R. W. Hoffman, in *Thin Films*, p. 99, American Society for Metals, Metals Park, OH (1963).
9. A. Brenner and S. Senderoff, *J. Res. NBS*, **42**, 105 (1949).
10. C. H. Hsueh and A. G. Evans, *J. Appl. Phys.*, **54**, 6672 (1983).
11. W. Pompe and H. J. Weiss, in *Current Topics in Material Science*, Vol. 12, E. Kaldis, Editor, p. 231, North-Holland, Amsterdam (1985).
12. G. P. Cherepanov, in *Mechanics of Brittle Fracture*, McGraw-Hill, Inc., New York (1979).
13. O. Teschke and M. U. Kleinke, *This Journal*, **139**, 136 (1992).
14. S. P. Timoshenko and J. M. Gere, *Theory of Elastic Stability*, 2nd ed., McGraw-Hill-Kogakusha, Tokyo (1961).
15. A. G. Evans and J. W. Hutchinson, *Int. J. Solids Structures*, **20**, 455 (1984).

Theoretical Aspects of Potential Modulation Normal Incidence Reflection Absorption UV-Visible Spectroscopy under Forced Convection

Ming Zhao* and Daniel A. Scherson**

Department of Chemistry, Case Western Reserve University, Cleveland, Ohio 44106

ABSTRACT

A theoretical treatment is presented for the quantitative analysis of potential-modulated normal-incidence reflection absorption UV-visible spectra of solution-phase, optically absorbing species produced at the surface of a rotating disk electrode (RDE). This novel technique is based on the application of a sinusoidal voltage of small amplitude to the RDE to generate in turn, a perturbation in the concentration profile of the absorbing species, C. Such changes introduce a modulation in the absorptivity of the solution along the axis of rotation of the RDE, and these can be monitored by (near)-normal-incidence UV-visible reflection absorption spectroscopy. A mathematical analysis of the optics and hydrodynamics for the system indicates that the ratio (I^*/I_{dc}), where I^* is the amplitude of the ac and I_{dc} the magnitude of the dc components of the optical signal, is proportional to the extinction coefficient of C and to the absolute value of the integral of the time-independent function of the oscillatory concentration profile. Excellent agreement was obtained between the approximate solutions (in terms of the eigenfunctions, eigenvalues, and coefficients of the appropriate Sturm-Liouville system) valid in a domain of frequencies low enough to achieve optimum sensitivity and those determined by rigorous numerical integration of the governing differential equation subject to the appropriate boundary conditions. This provides a means of extracting quantitative information from the experimental data based on a simple mathematical expression.

The development of *in situ* spectroelectrochemical techniques in the presence of convective flow is expected to provide insight into the nature of intermediates and products of a variety of electrochemical reactions and thus shed light into mechanistic aspects of processes of technological and fundamental importance, including electrodeposition and electrocatalysis.^{1,2} Modulation strategies involving such variables as the electrode potential,³ the rotation rate of a disk electrode,⁴ and the wavelength of the incident

light⁵ can markedly increase the sensitivity of many of these methods. Despite these advantages, no attempts have yet been made to combine modulation and *in situ* spectroscopic techniques under well-defined hydrodynamic conditions.

This work will present theoretical aspects of potential-modulated normal-incidence UV-visible reflection absorption spectroscopy at a rotating disk electrode (RDE). As will be shown, the mathematical equations that relate the observed optical signal to the actual spectra of species present in the diffusion boundary layer can be expressed in

* Electrochemical Society Student Member.

** Electrochemical Society Active Member.